DOI: 10.1002/ejic.200600111

A Ruthenium(II) Complex with a Tripodal Ligand Containing Three Imidazole Groups

Tomoka Yamaguchi,[a] Kazutoshi Harada,[a] Yukinari Sunatsuki,[a] Masaaki Kojima,*[a] Kiyohiko Nakajima,[b] and Naohide Matsumoto[c]

Keywords: Ruthenium/ Redox chemistry / Chirality / Schiff bases / N ligands / Tripodal ligands

The orange $[Ru^{II}(H_3L)](ClO_4)_2 \cdot 3H_2O$ (**1**) complex was synthesized from *cis*-$[RuCl_2(dmso)_4]$ and H_3L, where H_3L (tris{[2-{(imidazol-4-yl)methylidene}amino]ethyl}amine) is a tripodal ligand obtained by condensation of tris(2-aminoethyl)-amine and 4-formylimidazole in a 1:3 mol ratio. The X-ray crystal structure analysis revealed that the complex has an octahedral structure coordinated by three imidazole nitrogen atoms and three Schiff base (imine) nitrogen atoms. The uncoordinated NH groups of the imidazole moieties of **1** are easily deprotonated by the action of a base. The effect of deprotonation on the Ru^{III}/Ru^{II} redox potential was studied by cyclic voltammetry in methanol containing 0.1 M $LiClO_4$. Complete deprotonation shifts the Ru^{III}/Ru^{II} potential to a much more negative value from –0.18 to –0.72 V vs. Ag/Ag^+, making it easier to oxidize. The bluish-purple Ru^{III} complex, $[Ru^{III}(H_3L)]^{3+}$, was formed by controlled-potential electrolysis of **1**, and the electronic spectrum is reported.

Introduction

Ruthenium complexes containing imidazole and its derivatives have attracted great attention in recent years since several of them serve as antitumor drugs.[1] For example, $(H_2im)[Ru^{III}Cl_4(Him)(dmso)]$ (Him = imidazole) and $(H_2ind)[Ru^{III}Cl_4(Hind)(dmso)]$ (Hind = indazole) are on clinical trials, the first as an antimetastatic drug and the second as an anticancer agent against primary tumors and metastases and, in particular, colon carcinomas. As a mode of antitumor action of the Ru^{III} complexes, the "activation by reduction" hypothesis was proposed. The Ru^{III} complexes were suggested to serve as prodrugs that are activated by reduction to Ru^{II} in order to coordinate more rapidly to biomolecules.[1d] In other words, the Ru^{III} complexes should possess biologically accessible reduction potentials to be active in vivo.

Recently, we reported the structures and properties of Fe^{II} and Fe^{III} complexes with a tripodal ligand containing three imidazole groups, H_3L; H_3L (tris{[2-{(imidazol-4-yl)methylidene}amino]ethyl}amine) is a potentially heptadentate Schiff-base ligand derived from 1:3 condensation of tris(2-aminoethyl)amine and 4-formylimidazole (Figure 1).[2] The X-ray crystal structure analysis of $[Fe^{II}(H_3L)](BF_4)_2 \cdot 3H_2O$ revealed that the Fe^{II} ion is surrounded by three Schiff base (imine) nitrogen and three imidazole nitrogen atoms in an octahedral fashion, where the tertiary amine nitrogen atom is uncoordinated. The uncoordinated imidazole NH hydrogen atoms of $[Fe^{II}(H_3L)]^{2+}$ are easily deprotonated; upon addition of up to three equiv. of NaOH, $[Fe^{II}(H_3L)]^{2+}$ in methanol under aerobic conditions shows a drastic color change from yellowish-orange, through reddish-orange and green, to deep blue.[2c] Fe^{II} species are oxidized to Fe^{III} by air under basic conditions, and from the final blue solution, we obtained the iron(III) complex, $[Fe^{III}(L)]$, containing the deprotonated ligand L^{3-}. Deprotonation of $[Fe^{II}(H_3L)]^{2+}$ induces oxidation of the metal center to generate the $[Fe^{III}(L)]^0$ species. Thus, this reaction is an example of a proton-coupled electron-transfer (PCET) reaction.[3] If we study a ruthenium complex with a ligand containing several imidazole groups such as H_3L, we should be able to control the redox potential by adjusting the pH of the solution because the complex will have several different pK_a values. PCET is the basic mechanism of bioenergetic conversion. Small-molecule activation, redox-driven proton pumps, and hydrogen atom abstraction reactions of a wide variety of oxidases and reductases all involve the coupling of electrons to protons.[1d] Thus, $[Ru^{II}(H_3L)]^{2+}$ should be an ideal system to study the pH-dependent metal-based couples as models for PCET reactions because deprotonation should affect the stability of the oxidation state of the Ru complex.

We report here the synthesis, structure, and properties of a Ru^{II} complex with a tripodal ligand containing three

[a] Department of Chemistry, Faculty of Science, Okayama University,
Tsushima-naka 3-1-1, Okayama 700-8530, Japan
Fax: +81-86-251-7842
E-mail: kojima@cc.okayama-u.ac.jp
[b] Department of Chemistry, Aichi University of Education, Kariya, Aichi 448-8542, Japan
[c] Department of Chemistry, Faculty of Science, Kumamoto University,
Kurokami 2-39-1, Kumamoto 860-8555, Japan

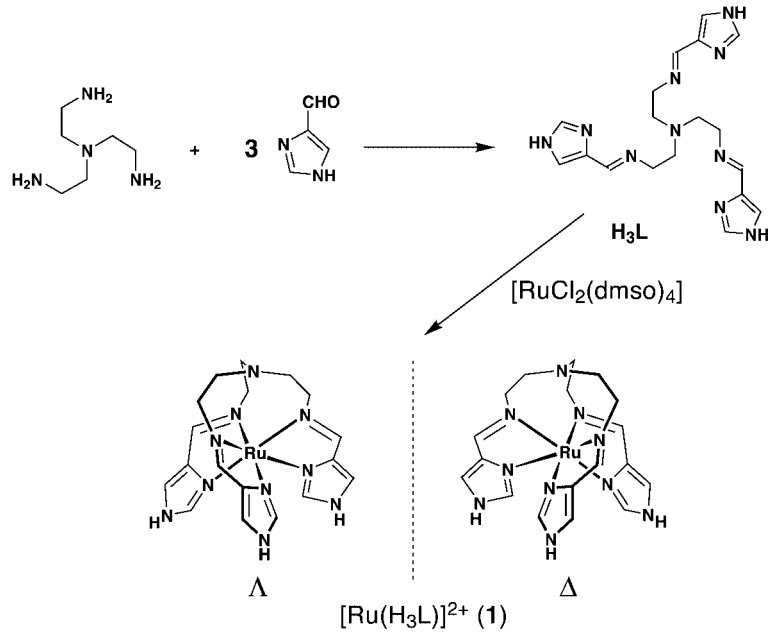

Figure 1. Synthetic procedures for the tripodal H_3L ligand and $[Ru^{II}(H_3L)]^{2+}$ (**1**), and the Δ and Λ configurations of complex **1**.

imidazole groups, $[Ru(H_3L)](ClO_4)_2$ (Figure 1), with emphasis being placed on the effect of deprotonation on the cyclic voltammogram (CV) and on the electronic spectrum.

Results and Discussion

Synthesis and Characterization

The tripodal H_3L ligand was prepared by the condensation reaction of tris(2-aminoethyl)amine and 4-formylimidazole in a 1:3 mol ratio in methanol (Figure 1). The H_3L ligand was not isolated and a solution containing this ligand was used for the synthesis of $[Ru(H_3L)](ClO_4)_2\cdot 3H_2O$ (**1**). Orange $[Ru(H_3L)]^{2+}$ was prepared by mixing the ligand and *cis*-$[RuCl_2(dmso)_4]$[4] in a 10:1 mol ratio. It should be noted that the ligand/$[RuCl_2(dmso)_4]$ ratio is not 1.0, but 10. We tried to prepare the complex in different ligand/Ru ratios. A large excess of the ligand seems to be necessary to yield the desired complex. At present, we cannot explain why complex **1** does not form under the equivalent mol ratio (ligand/Ru = 1.0).

The IR spectrum of complex **1** ($4d^6$, t_{2g}^6) shows an intense band assignable to the Cl–O vibration of the perchlorate ion at 1088–1143 cm^{-1} and an intense characteristic absorption at 1607 cm^{-1} assignable to the C=N stretching vibration of the tripodal Schiff-base ligand. The position of the C=N stretching band is close to that of $[Fe^{II}(H_3L)](BF_4)_2\cdot 3H_2O$ (1610 cm^{-1}) in the low-spin state ($3d^6$, t_{2g}^6).[2f] It has been reported that the position of the C=N stretching band is sensitive to the electronic state of the complex. For example, $[Fe^{II}(H_3L)](BF_4)_2\cdot 3H_2O$ exhibits a spin crossover behavior and the high-spin species ($t_{2g}^4e_g^2$) shows the C=N stretching vibration in the Raman spectrum at a higher energy (1638 cm^{-1}, $T > 200$ K) than the low-spin one (1610 cm^{-1}, $T < 100$ K).[2f] Complex **1** in D_2O shows a very simple ^1H NMR spectrum, and it conforms to the high symmetry (C_3) of the complex confirmed by X-ray crystallography.

Crystal Structure

The crystal structure consists of a ruthenium(II) complex cation, $[Ru(H_3L)]^{2+}$, and two perchlorate ions as the counteranions. Figure 2 shows an ORTEP drawing of the cation of complex **1** with the atom numbering scheme. Selected distances and angles, with their estimated standard deviations in parentheses, are listed in Table 1. A ruthenium(II) ion with the $4d^6$, t_{2g}^6 electron configuration assumes an octahedral coordination environment with the N_6 donor set of the tripodal ligand including three imidazole and three Schiff base nitrogen atoms. The tertiary amine nitrogen atom (N1) is not coordinated, the Ru···N1 distance being 3.161(6) Å. The lengths of the six Ru–N bonds are 2.151(7)–2.232(8) Å, and are in the expected range for the given coordination number and donor atoms. The corresponding M–N bond lengths for $[Co^{III}(H_3L)](ClO_4)_3\cdot H_2O$ ($3d^6$, t_{2g}^6) and $[Fe^{II}(H_3L)](BF_4)_2\cdot 3H_2O$ ($3d^6$, t_{2g}^6) are as follows: Co^{III} 1.88(1)–1.98(1) Å,[5] Fe^{II} 1.981(3)–1.989(4) Å.[2f] Ionic radii (Shannon) for six-coordinate Co^{III} and Fe^{II} are reported to be 0.69 and 0.75 Å, respectively.[6] The ionic radius (Shannon) for Ru^{II} is not available. However, on the basis of the above M–N bond lengths, we can estimate the ionic radius for Ru^{II} to be ca. 0.95 Å, assuming the nature of the bonding is similar for each one of the three complexes.

The crystal consists of a dimeric unit. Two adjacent complex cations with the opposite absolute configurations (Δ and Λ) are connected in a tail-to-tail fashion by N–H···O(ClO_4^-)···H–N hydrogen bonds through two counter-ClO_4^- anions, with N(imidazole)···O(ClO_4^-) dis-

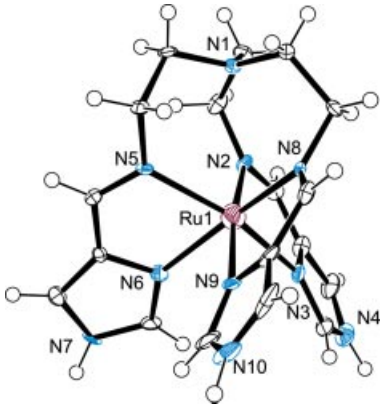

Figure 2. ORTEP drawing of the cation of $[Ru(H_3L)](ClO_4)_2$ (**1**) with atom numbering scheme showing the 50% probability ellipsoids.

tances of 3.01(1) and 2.96(1) Å and the N(imidazole)···O(ClO_4^-)···N(imidazole) angle of 102.0(3)° (Figure 3, Table 2). Each of the other two flanking ClO_4^- ions in Figure 3 (part a) are hydrogen-bonded with only one complex cation.

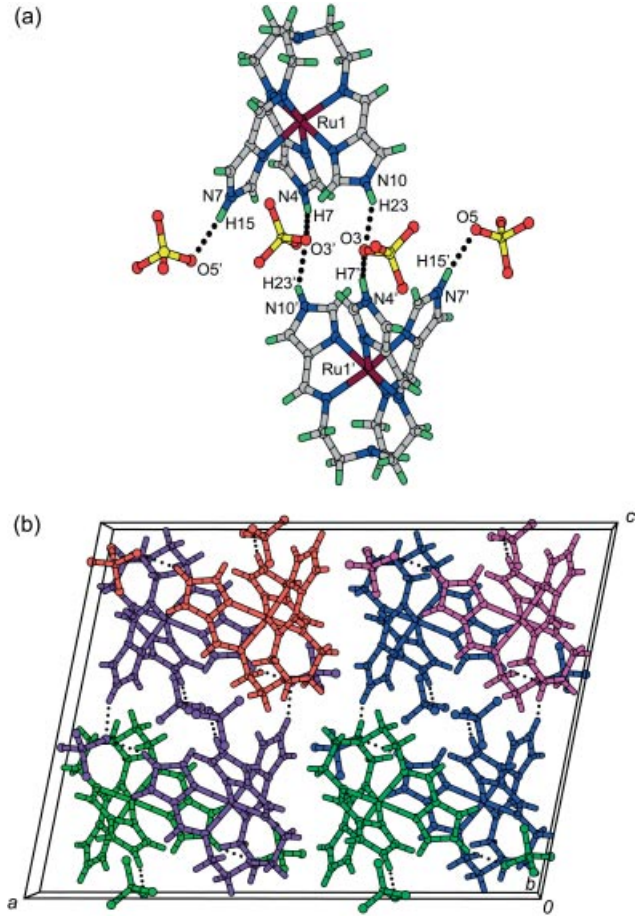

Figure 3. X-ray crystal structure of $[Ru(H_3L)](ClO_4)_2$ (**1**). (a) Two ClO_4^- ions connect the two adjacent complex cations through hydrogen bonding, while the other two flanking ClO_4^- ions are hydrogen bonded with only one complex cation. (b) Crystal packing showing that the two complex cations in the same color are connected by hydrogen bonding.

Table 1. Selected distances [Å] and angles [°] for $[Ru(H_3L)](ClO_4)_2$ (**1**).[a]

Bond lengths			
Ru(1)–N(2)	2.172(8)	Ru(1)–N(3)	2.190(7)
Ru(1)–N(5)	2.194(7)	Ru(1)–N(6)	2.190(8)
Ru(1)–N(8)	2.151(7)	Ru(1)–N(9)	2.232(8)
Interatomic distances			
Ru(1)···N(1)	3.161(6)	Ru(1)···Ru(1)^1	7.646(1)
Ru(1)^1···Ru(1)^2	7.453(1)	Ru(1)^1···Ru(1)^3	10.197(1)
Bond angles			
N(3)–Ru(1)–N(2)	77.6(3)	N(5)–Ru(1)–N(2)	96.7(3)
N(6)–Ru(1)–N(2)	92.6(3)	N(8)–Ru(1)–N(2)	102.6(3)
N(9)–Ru(1)–N(2)	173.0(3)	N(5)–Ru(1)–N(3)	162.5(3)
N(6)–Ru(1)–N(3)	86.7(3)	N(8)–Ru(1)–N(3)	100.5(3)
N(9)–Ru(1)–N(3)	95.6(3)	N(6)–Ru(1)–N(5)	77.0(3)
N(8)–Ru(1)–N(5)	96.9(3)	N(9)–Ru(1)–N(5)	90.3(3)
N(9)–Ru(1)–N(6)	88.8(3)	N(9)–Ru(1)–N(8)	76.6(3)

[a] Symmetry operators: (1) $1/2-x$, $1/2+y$, $1/2-z+1$; (2) $1/2+x$, $1/2+y$, $+z$; (3) $+x$, $-y+1$, $1/2+z-1$.

Table 2. Intermolecular hydrogen bond lengths [Å] and angles [°] for $[Ru(H_3L)](ClO_4)_2$ (**1**).

D	H	A	D···A	D–H	H···A	D–H···A
N(4)	H(7)	O(3′)[a]	3.01(1)	0.95(1)	2.13(1)	154(1)
N(10)	H(23)	O(3)[b]	2.96(1)	0.95(1)	2.12(1)	147(1)
N(7)	H(15)	O(5′)[c]	3.01(1)	0.950(9)	2.07(1)	167.1(8)

[a] $1/2-x$, $1/2+y$, $3/2-z$. [b] $+x$, $-y$, $1/2+z$. [c] $+x$, $-1+y$, z.

Electronic and CD Spectra

The electronic spectrum of complex **1** in methanol is shown in Figure 4. The complex is fairly stable in methanol under aerobic conditions and the spectrum stays unchanged for at least five hours. The complex shows an intense band attributable to a metal-to-ligand charge transfer (MLCT) transition in the visible region at 424 nm (13900 $M^{-1}cm^{-1}$), which obscures the weak d–d bands. The MLCT band is unsymmetrical, which may be related to the less than octahedral local symmetry (C_3) of the complex that leads to loss of the degeneracy of the MLCT transitions. The bands in the UV region are mainly due to intraligand transitions. The electronic spectrum of the H_3L ligand in methanol is also shown in Figure 4. Comparison of the two spectra indicates that the shoulder around 330 nm of **1** is attributable to the Schiff base π–π* transition and that the intense band at 248 nm is mainly due to the imidazole moiety.

The uncoordinated NH groups of the imidazole moieties of **1** can be deprotonated by the action of a base. With the addition of $NaOCH_3$ to $[Ru(H_3L)]^{2+}$ in methanol, a slight color change from yellow to yellowish-orange was observed: aliquots of the methanolic $NaOCH_3$ solution were added up to three equiv. to $[Ru(H_3L)]^{2+}$ in methanol, and the reaction was followed spectrophotometrically (Figure 5). Although isosbestic points were observed at 375 and 440 nm, the latter is not sharp. This behavior can be ex-

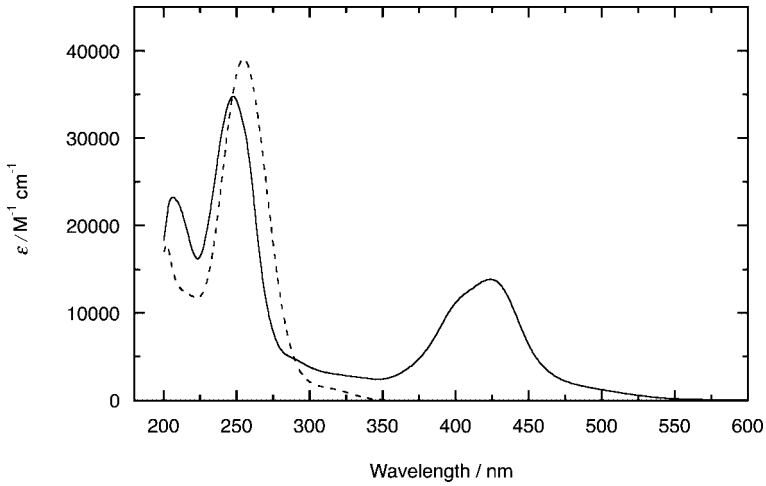

Figure 4. Electronic spectra of $[Ru(H_3L)](ClO_4)_2 \cdot 3H_2O$ (**1**, ——) and the H_3L ligand (- - -) in methanol.

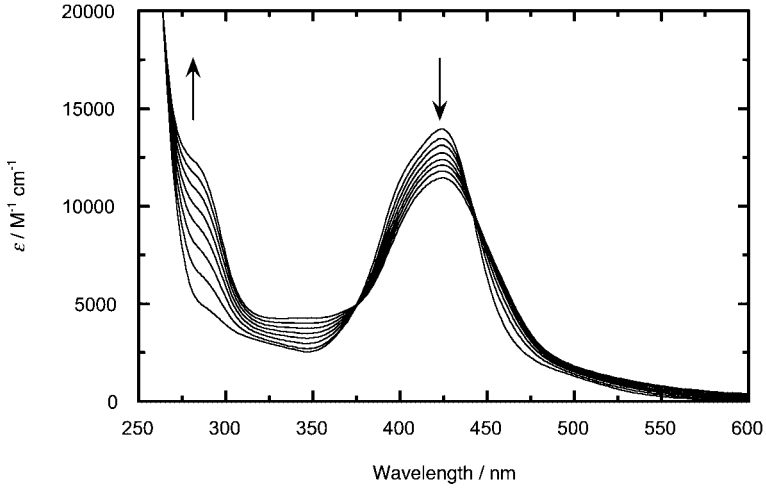

Figure 5. Electronic spectral changes of $[Ru(H_3L)](ClO_4)_2 \cdot 3H_2O$ (**1**) upon addition of $NaOCH_3$. $NaOCH_3$ in methanol was added stepwise to a methanol solution of **1** (3.4×10^{-5} M) up to 3.0 equiv.

plained as follows : The pK_a values for $[Ru(H_3L)]^{2+}$, $[Ru(H_2L)]^{+}$, and [Ru(HL)] are similar to each other, and many species ($[Ru^{II}(H_3L)]^{2+}$, $[Ru^{II}(H_2L)]^{+}$, $[Ru^{II}(HL)]^{0}$, and $[Ru^{II}(L)]^{-}$) exist in equilibrium to obscure the isosbestic points [Equation (1)].

$$[Ru^{II}(H_3L)]^{2+} \underset{-H^+}{\overset{+H^+}{\leftrightarrows}} [Ru^{II}(H_2L)]^{+} \underset{-H^+}{\overset{+H^+}{\leftrightarrows}} [Ru^{II}(HL)] \underset{-H^+}{\overset{+H^+}{\leftrightarrows}} [Ru^{II}(L)]^{-} \quad (1)$$

In order to examine the stability of the deprotonated species under aerobic conditions, we measured the spectral change with the passage of time. After the addition of one equiv. of $NaOCH_3$, the spectrum stayed almost unchanged for at least 90 min. However, with the addition of two equiv. of $NaOCH_3$, a slight spectral change was observed after 90 min. This spectral change may be due to oxidation of Ru^{II} to Ru^{III}. This behavior is in agreement with the cyclic voltammetry results described later. Thus, the above deprotonation reaction was carried out under an inert atmosphere. The reaction is reversible: protonation of $[Ru^{II}(L)]^{-}$ in methanol takes place upon sequential addition of $HClO_4$ in methanol, and the complex is finally converted to $[Ru^{II}(H_3L)]^{2+}$ [Equation (1)].

$[Ru(H_3L)]^{2+}$ is chiral because of a spiral coordination arrangement of the achiral H_3L ligand around the Ru^{II} ion. Optical resolution was carried out by column chromatography on SP-Sephadex, with 0.15 M sodium (+)-tartrate being used as the eluent.[7] The eluate was collected fractionally. The first and last fractions show CD patterns that are enantiomeric to each other, as shown in Figure 6. A strong CD band around 330 nm is attributable to the Schiff base π–π* transition. Recently, we have reported that the Fe^{II} complex containing the H_3L ligand, $[Fe^{II}(H_3L)](BF_4)_2 \cdot 3H_2O$, is spontaneously resolved, and X-ray crystallography revealed that the complex showing negative CD around 320 nm, attributable to the Schiff base π–π* transition, has the Δ absolute configuration.[2f] We have also resolved

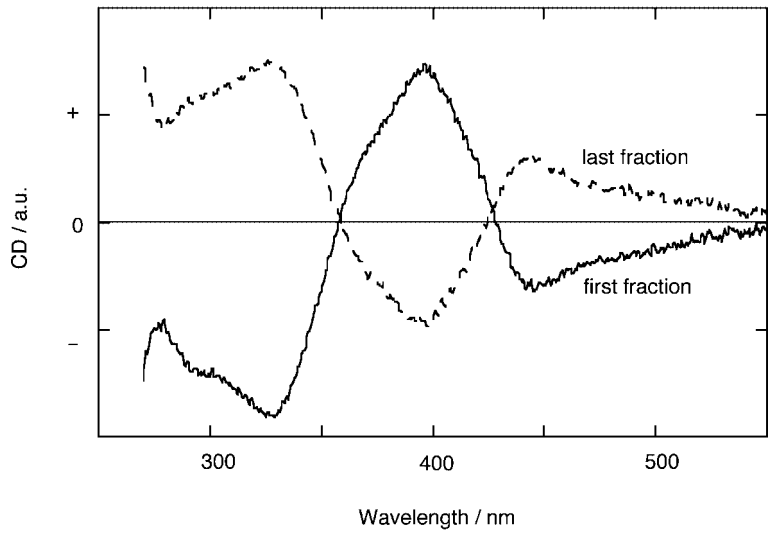

Figure 6. Circular dichroism (CD) spectra of $[Ru^{II}(H_3L)]^{2+}$ (**1**) resolved by SP-Sephadex column chromatography [eluent: 0.15 M Na_2(+)-tart], the first (——) and the last (- - -) fraction showing patterns that are enantiomeric to each other.

$[Co^{III}(H_2L)]^{2+}$ by fractional crystallization of the diastereomeric salt with $[Sb_2\{(+)\text{-tart}\}_2]^{2-}$ [tart = tartrate(4) ion] and have determined the absolute configuration by X-ray crystallography.[8] The less soluble diastereomeric salt, $[Co^{III}(H_2L)][Sb_2\{(+)\text{-tart}\}_2]\cdot 4H_2O$, has the Λ configuration and exhibits positive CD around 320 nm. From these results, we conclude that the faster-eluted enantiomer of $[Ru(H_3L)]^{2+}$ showing negative CD around 330 nm has the Δ absolute configuration. Exciton theory has been applied to tris(chelate)- or *cis*-bis(chelate)-type metal complexes, where chelate denotes such ligands as 2,2-bipyridine, 1,10-phenanthroline, or Schiff-base ligands, and the relationship between the CD pattern in the ligand π–π* transition region and the absolute configuration around the metal ion has been established.[9] The conclusion described above for the present complex is in agreement with the assignment based on exciton theory.

Electrochemistry

The electrochemical properties of $[Ru^{II}(H_3L)]^{2+}$ and its deprotonated forms, $[Ru^{II}(H_2L)]^{+}$, $[Ru^{II}(HL)]^{0}$, and $[Ru^{II}(L)]^{-}$, were studied by cyclic voltammetry (CV). The measurements were performed under nitrogen using methanol solutions containing $LiClO_4$ (0.1 M) as the supporting electrolyte. The redox couple of $[Ru^{II}(H_3L)]^{2+}$ appears at –0.18 V (E_{pc} = –0.21 V, E_{pa} = –0.15 V) vs. Ag/Ag^+ irrespective of the scan rate ($10 \leq v \leq 200$ mV s^{-1}), the peak current ratio i_{pa}/i_{pc} was found to be 1.0, (i_{pa} or i_{pc})/$v^{1/2}$ was independent of v, and the peak separation (ΔE_p) was 0.060 V (Figure 7). These results are consistent with an electrochemically reversible one-electron redox process, see Equation (2).

$$[Ru^{III}(H_3L)]^{3+} + e^- \leftrightarrows [Ru^{II}(H_3L)]^{2+} \quad (2)$$

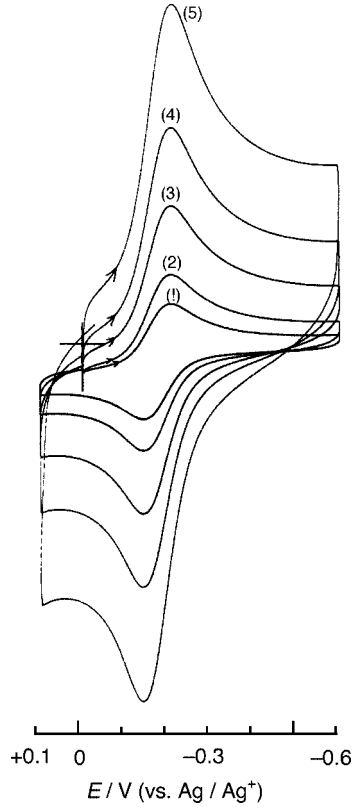

Figure 7. Cyclic voltammograms of $[Ru(H_3L)](ClO_4)_2\cdot 3H_2O$ (**1**, 0.2 mM) in methanol containing 0.1 M $LiClO_4$ at a glassy carbon electrode at sweep rates of (1) 10, (2) 20, (3) 50, (4) 100, and (5) 200 mV s^{-1}.

The bluish-purple Ru^{III} complex, $[Ru^{III}(H_3L)]^{+}$, was formed by controlled-potential electrolysis of $[Ru^{II}(H_3L)]^{2+}$ at 0.0 V vs. Ag/Ag^+ in methanol containing 0.1 M (n-$C_4H_9)_4NBF_4$. The progress of the oxidation reaction was monitored spectrophotometrically (Figure 8). The band at

424 nm decreased while two bands appeared at 320 and 580 nm, and isosbestic points were observed at 370 and 480 nm. The broad moderately intense band at 580 nm can be assigned as an LMCT band.[10]

$[Ru^{II}(H_3L)]^{2+}$ in methanol undergoes reversible deprotonation and protonation upon addition of a base and an acid, respectively, as described above (deprotonation–protonation is associated with the imidazole moieties). Figure 9 shows the progress of the deprotonation reaction as monitored by cyclic voltammetry. Upon addition of one equiv. of $NaOCH_3$ to $[Ru^{II}(H_3L)]^{2+}$ in methanol (Figure 9, b), the current intensity of the initial redox couple at –0.18 V (E_{pc} = –0.21 V, E_{pa} = –0.15 V; Figure 9, a) diminishes and the couple shifts slightly to a more negative potential (E_{pc} = –0.29 V, E_{pa} = –0.18 V), and a new redox couple attributable to $[Ru^{III/II}(H_2L)]^{2+/+}$ appears at –0.67 V (E_{pc} = –0.72 V, E_{pa} = –0.61 V). Upon addition of one more equiv. of $NaOCH_3$ (Figure 9, c), the second redox couple shifts to a more negative potential (E_{pc} = –0.75 V, E_{pa} = –0.62 V) and grows at the expense of the first redox couple, and the initial redox couple shifts to a more negative potential (E_{pc} = –0.35 V, E_{pa} = –0.24 V). Full deprotonation at the imidazolate nitrogen moieties is achieved by adding three equiv. of base to produce $[Ru^{II}(L)]^{-}$ (see part d in Figure 9, $E^{0\prime}$ = –0.72 V, E_{pc} = –0.77 V, E_{pa} = –0.66 V). Complete deprotonation of the ligand shifts the Ru^{III}/Ru^{II} redox potential to a more negative value from –0.18 V to –0.72 V, i.e. 180 mV per proton. Carina et al.[11] reported that deprotonation of the uncoordinated NH groups of the imidazole moieties switches the redox potential of iron by as much as 345 mV per proton. A series of reverse reactions was observed when an acid (HCl) was added to $[Ru^{II}(L)]^{-}$. These results are consistent with the acid–base equilibrium [Equation (1)]. Analysis of the CVs in Figure 9 (a–d), suggests that each $[Ru^{II}(H_{3-n}L)]^{(2-n)+}$ (n = 0–3) species is characterized by a different potential of the redox couple although the redox couple for $[Ru^{III/II}(HL)]^{+/0}$ was not clearly observed; as the degree of deprotonation increases, the redox potential becomes more negative (i.e. the compound becomes easier to oxidize). These results are in accordance with the instability of the deprotonated species under aerobic conditions, as observed by electronic spectroscopy. It is worth noting that, for a metal complex with a ligand exhibiting acid–base properties in aqueous solution, the redox potential value is pH dependent; usually, however, each species (fully deprotonated, monodeprotonated, etc.) does not show an independent redox couple, but only an averaged couple is observed.[12] The $[Ru^{II}(L)]^{-}$ species exhibits another redox couple at +0.12 V (Figure 9d, E_{pc} = +0.08 V,

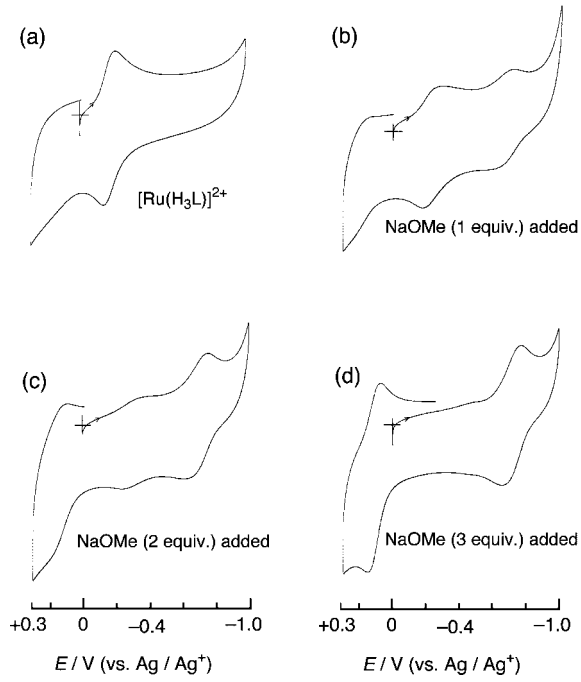

Figure 9. Progress of the deprotonation of $[Ru(H_3L)](ClO_4)_2{\cdot}3H_2O$ as monitored by cyclic voltammetry. (a)–(d): stepwise addition (0, 1, 2, and 3 equiv.) of $NaOCH_3$ in methanol to 0.2 mM $[Ru(H_3L)](ClO_4)_2{\cdot}3H_2O$ in methanol containing $LiClO_4$ (0.1 M).

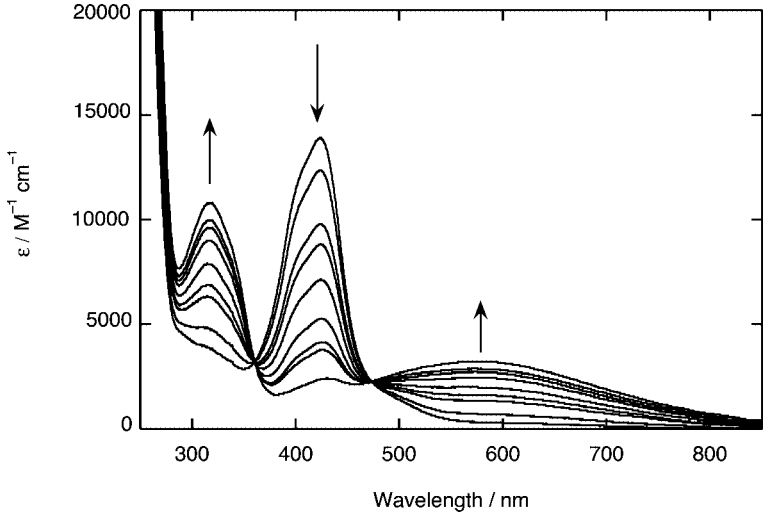

Figure 8. Electronic spectral changes accompanied by the progress of controlled-potential electrolysis (oxidation) of $[Ru(H_3L)]^{2+}$ in methanol containing 0.1 M $(n\text{-}C_4H_9)_4NBF_4$ at 0.0 V vs. Ag/Ag^+.

E_{pa} = +0.16 V), and this couple may be assigned as the $Ru^{IV/III}$ process.[10]

We have demonstrated that the uncoordinated NH groups of the imidazole moieties of **1** can easily be deprotonated by the action of a base, and that deprotonation stabilizes the oxidized form, Ru^{III}.

Experimental Section

Caution! Perchlorate salts of metal complexes are potentially explosive. Only small quantities of material should be prepared, and the samples should be handled with care.

Materials: All reagents and solvents in the syntheses were of reagent grade and were used without further purification. *cis*-$[RuCl_2(dmso)_4]$ was prepared according to the literature procedure.[4]

$[Ru(H_3L)](ClO_4)_2\cdot 3H_2O$ (1): A methanol solution (20 cm^3) containing tris(2-aminoethyl)amine (0.73 g, 5 mmol) and 4-formylimidazole (1.44 g, 15 mmol) was heated under reflux for 20 min to give a yellow-orange solution. This methanol solution contains the H_3L ligand, and the solution was used for the preparation of the Ru complex. Nitrogen (or argon) gas was bubbled through the solution for 15 min to remove oxygen (Solution A). *cis*-$[RuCl_2(dmso)_4]$ (0.242 g, 0.5 mmol) was dissolved in oxygen-free methanol (20 cm^3), and the ligand solution (Solution A) was added to this solution by a syringe. The mixture was heated under reflux for 6 h. The color of the solution changed from orange to dark brown. The solution was cooled to room temperature, and a methanol solution (50 cm^3) of NH_4BF_4 (1.6 g, 15 mmol) was added to give a brown precipitate, which was collected by filtration. This product is not soluble in common organic solvents, and it is not the desired compound, but seems to be an oligomer. The filtrate was diluted with 0.01 M HCl (300 cm^3). The solution was passed through a column (2.7 cm I.D. × 15 cm) of SP-Sephadex C-25. The adsorbed cationic species were eluted with 0.2 M NaCl/0.01 M HCl. The eluate containing the fastest eluted orange-red band was collected, and mixed with an aqueous solution (5 cm^3) of $NaClO_4$ (0.2 g). The orange crystals that deposited were collected by filtration. They were recrystallized from water under nitrogen. Yield 15 mg. $C_{18}H_{30}Cl_2N_{10}O_{11}Ru_1$ = $[Ru(H_3L)](ClO_4)_2\cdot 3H_2O$: calcd. C 29.44, H 4.11, N 19.07; found C 29.34, H 3.74, N 18.88. ^1H NMR (D_2O, ref. DSS): δ = 2.8–3.5 (m, 4 H, CH_2), 7.25 (s, 1 H), 7.80 (s, 1 H), 8.52 (s, 1 H) ppm. IR (KBr pellet): $\tilde{\nu}$ = $\nu_{C=N}$(Schiff base), 1607 cm^{-1}; $\nu_{Cl-O}(ClO_4^-)$, 1088, 1115, 1143 cm^{-1}. UV/Vis (CH_3OH): λ (ε) = 424 nm (13900 M^{-1} cm^{-1}), 248 nm (34800 M^{-1} cm^{-1}). Crystals suitable for X-ray analysis were obtained by adding a diethyl ether layer to an acetonitrile solution of the complex.

Optical Resolution: An aqueous solution (20 cm^3) of $[Ru(H_3L)](ClO_4)_2\cdot 3H_2O$ (3 mg) was adsorbed onto SP-Sephadex (1 cm^3) and the SP-Sephadex was placed on top of an SP-Sephadex column (1 cm ID × 30 cm). The complex was eluted with 0.15 M sodium (+)-tartrate, and the eluate was fractionally collected.[7]

Physical Measurements: UV/Vis absorption spectra were recorded with a JASCO Ubest-550 spectrophotometer. Infrared spectra were measured on a JASCO FT/IR-550 spectrophotometer. CD spectra were recorded with a JASCO J-720 spectropolarimeter. ^1H NMR spectra were recorded with a Varian Mercury 300 spectrometer (^1H at 300 MHz) at ambient temperature. Cyclic voltammetry measurements were performed under nitrogen using a Fuso HECS 321B potential sweep unit with methanol solutions containing $LiClO_4$ (0.1 M) as the supporting electrolyte. The electrochemical cell was a three-electrode system consisting of a glassy-carbon working electrode, a platinum wire auxiliary electrode, and an Ag/Ag^+ (Ag/0.01 M $AgNO_3$) reference electrode. As an external standard, the Fc/Fc^+ (Fc = ferrocene) couple was observed at –0.170 V vs. Ag/Ag^+ under the same conditions. Controlled-potential electrolysis experiments were carried out with a platinum-gauze working electrode, with the use of a Fuso HECS 312B DC-pulse polarograph and a Model 1109 integrator. The reference electrode was the same Ag/Ag^+ (Ag/0.01 M $AgNO_3$) electrode used for the cyclic voltammetric experiments, and the auxiliary electrode was a platinum wire separated from the test solution by a salt bridge.

X-ray Data Collection, Reduction, and Structure Determination: An orange crystal of **1**, with the approximate dimensions 0.5 × 0.2 × 0.1 mm, was mounted by a loop method, and the X-ray data were collected with a Rigaku R-AXIS RAPID II imaging plate area detector using graphite-monochromated Mo-K_α radiation (λ = 0.71073 Å). The crystallographic data are summarized in Table 3. The structure was solved by direct methods, and was refined using full-matrix least-squares procedures with the CrystalStructure crystallographic software package.[13] There are two possible space groups, *C*2/*c* (No.15) and *Cc* (No.9). We tried to solve the structure in both space groups. Only the space group *C*2/*c* gave rational results.

Table 3. X-ray crystallographic data for $[Ru(H_3L)](ClO_4)_2$ (**1**).

Formula	$C_{18}H_{24}Cl_2N_{10}O_8Ru$
Formula mass [g mol^{-1}]	680.43
Crystal system	monoclinic
Space group	*C*2/*c* (No.15)
a [Å]	25.758(8)
b [Å]	10.772(4)
c [Å]	18.933(5)
α [°]	90
β [°]	101.57(1)
γ [°]	90
V [$Å^3$]	5146(2)
Z	8
D_{calcd} [g cm^{-3}]	1.756
μ [cm^{-1}]	8.82
R_1[a] [$I > 2.0\sigma(I)$]	0.082
wR_2[b] [all data]	0.243
T [°C]	–180

[a] $R_1 = \Sigma||F_o| - |F_c|| / \Sigma|F_o|$. [b] $wR_2 = \{\Sigma[w(F_o^2 - F_c^2)^2]/\Sigma w(F_o^2)^2\}^{1/2}$.

CCDC-298967 contains the supplementary crystallographic data for this paper. These data can be obtained free of charge from The Cambridge Crystallographic Data Centre via www.ccdc.cam.ac.uk/data_request/cif.

Acknowledgments

This work was supported in part by a Grant-in-Aid for Scientific Research (Nos. 17550056, 16205010, 16750050, and 17350028) from the Ministry of Education, Science, Sports, and Culture of Japan, and by the Iketani Science and Technology Foundation. T. Y. was supported by the JSPS program for Research Fellowships for Young Scientists (No. 17003601).

[1] a) E. Reisner, V. B. Arison, M. F. C. Guedes de Silva, R. Lichtenecker, A. Eichnger, B. K. Keppler, V. Yu. Kukushkin, A. J. L. Pombeiro, *Inorg. Chem.* **2004**, *43*, 7083–7093; b) A. Egger, V. B. Arison, E. Reisner, B. Cebrian-Losantos, S. Shova, G. Trettenhahm, B. K. Keppler, *Inorg. Chem.* **2005**, *44*, 122–, 132; c) E.

Reisner, V. B. Arison, A. Eichinger, N. Kandler, G. Giester, A. J. L. Pombeiro, B. K. Keppler, *Inorg. Chem.* **2005**, *44*, 6704–6716; d) M. J. Clarke, F. Zhu, D. R. Frasca, *Chem. Rev.* **1999**, *99*, 2511–2533; e) C. J. Chang, M. C. Y. Chang, N. H. Damrauer, D. G. Nocera, *Biochim. Biophys. Acta* **2004**, *1655*, 13–28; f) M. J. Clarke, *Coord. Chem. Rev.* **2003**, *236*, 209–233 and references cited therein.

[2] a) Y. Sunatsuki, Y. Ikuta, N. Matsumoto, H. Ohta, M. Kojima, S. Iijima, S. Hayami, Y. Maeda, S. Kaizaki, F. Dahan, J.-P. Tuchagues, *Angew. Chem. Int. Ed.* **2003**, *42*, 1614–1618; b) H. Ohta, Y. Sunatsuki, Y. Ikuta, N. Matsumoto, S. Iijima, H. Akashi, T. Kambe, M. Kojima, *Mater. Sci.* **2003**, *21*, 191–198; c) Y. Ikuta, M. Ooidemizu, Y. Yamahata, M. Yamada, S. Osa, N. Matsumoto, S. Iijima, Y. Sunatsuki, M. Kojima, F. Dahan, J.-P. Tuchagues, *Inorg. Chem.* **2003**, *42*, 7001–7017; d) M. Yamada, M. Ooidemizu, Y. Ikuta, S. Osa, N. Matsumoto, S. Iijima, M. Kojima, F. Dahan, J.-P. Tuchagues, *Inorg. Chem.* **2003**, *42*, 8406–8416; e) H. Ohta, Y. Sunatsuki, M. Kojima, S. Iijima, H. Akashi, N. Matsumoto, *Chem. Lett.* **2004**, *33*, 350–351; f) Y. Sunatsuki, H. Ohta, M. Kojima, Y. Ikuta, Y. Goto, N. Matsumoto, S. Iijima, H. Akashi, S. Kaizaki, F. Dahan, J.-P. Tuchagues, *Inorg. Chem.* **2004**, *43*, 4154–4171.

[3] S. J. Slattery, J. K. Blaho, J. Lehnes, K. A. Goldsby, *Coord. Chem. Rev.* **1998**, *174*, 391–416 and references cited therein.

[4] I. P. Evans, A. Spencer, G. Wilkinson, *J. Chem. Soc., Dalton Trans.* **1973**, 204–209.

[5] I. Katsuki, Y. Motoda, Y. Sunatsuki, N. Matsumoto, T. Nakashima, M. Kojima, *J. Am. Chem. Soc.* **2002**, *124*, 629–640.

[6] R. D. Shannon, *Acta Crystallogr., Sect. A* **1976**, *32*, 751–767.

[7] Y. Yoshikawa, K. Yamasaki, *Coord. Chem. Rev.* **1979**, *28*, 205–229.

[8] H. Nakamura, M. Fujii, T. Hamada, T. Yamaguchi, Y. Sunatsuki, N. Matsumoto, M. Kojima, to be published.

[9] a) B. Bosnich, A. T. Phillip, *J. Am. Chem. Soc.* **1968**, *90*, 6352–6359; b) J. Hidaka, B. E. Douglas, *Inorg. Chem.* **1964**, *3*, 1180–1184; c) J. W. Canary, C. S. Allen, *J. Am. Chem. Soc.* **1995**, *117*, 8484–8485; d) S. Zahn, J. W. Canary, *Angew. Chem. Int. Ed.* **1998**, *37*, 305–308; e) J. M. Castagnetto, J. W. Canary, *Chem. Commun.* **1998**, 203–204.

[10] a) S. Chakraborty, M. G. Walawalkar, G. K. Lahiri, *J. Chem. Soc., Dalton Trans.* **2000**, 2875–2883; b) S. Deoghoria, S. Sain, T. K. Karmakar, S. K. Bera, S. K. Chandra, *J. Indian Chem. Soc.* **2002**, *79*, 857–859.

[11] R. F. Carina, L. Verzegnassi, G. Bernardinelli, A. F. Williams, *Chem. Commun.* **1998**, 2681–2682.

[12] a) A. M. Bond, M. Haga, *Inorg. Chem.* **1986**, *25*, 4507–4514; b) W. Szulbinski, P. R. Warburton, D. H. Busch, N. W. Alcock, *Inorg. Chem.* **1993**, *32*, 297–302.

[13] *Crystal Structure Analysis Package*, Rigaku and MSC, **2001**.

Received: February 8, 2006
Published Online: June 28, 2006

